Supporting Information

Kinetics of RNA Refolding in Dynamic Equilibrium by ^{1}H-Detected ^{15}N Exchange NMR Spectroscopy

Philipp Wenter, *Geoffrey Bodenhausen*, *Jens Dittmer** and *Stefan Pitsch**

Contents:

1. Supporting Figure S1: HNN correlation experiments for duplex/hairpin discrimination

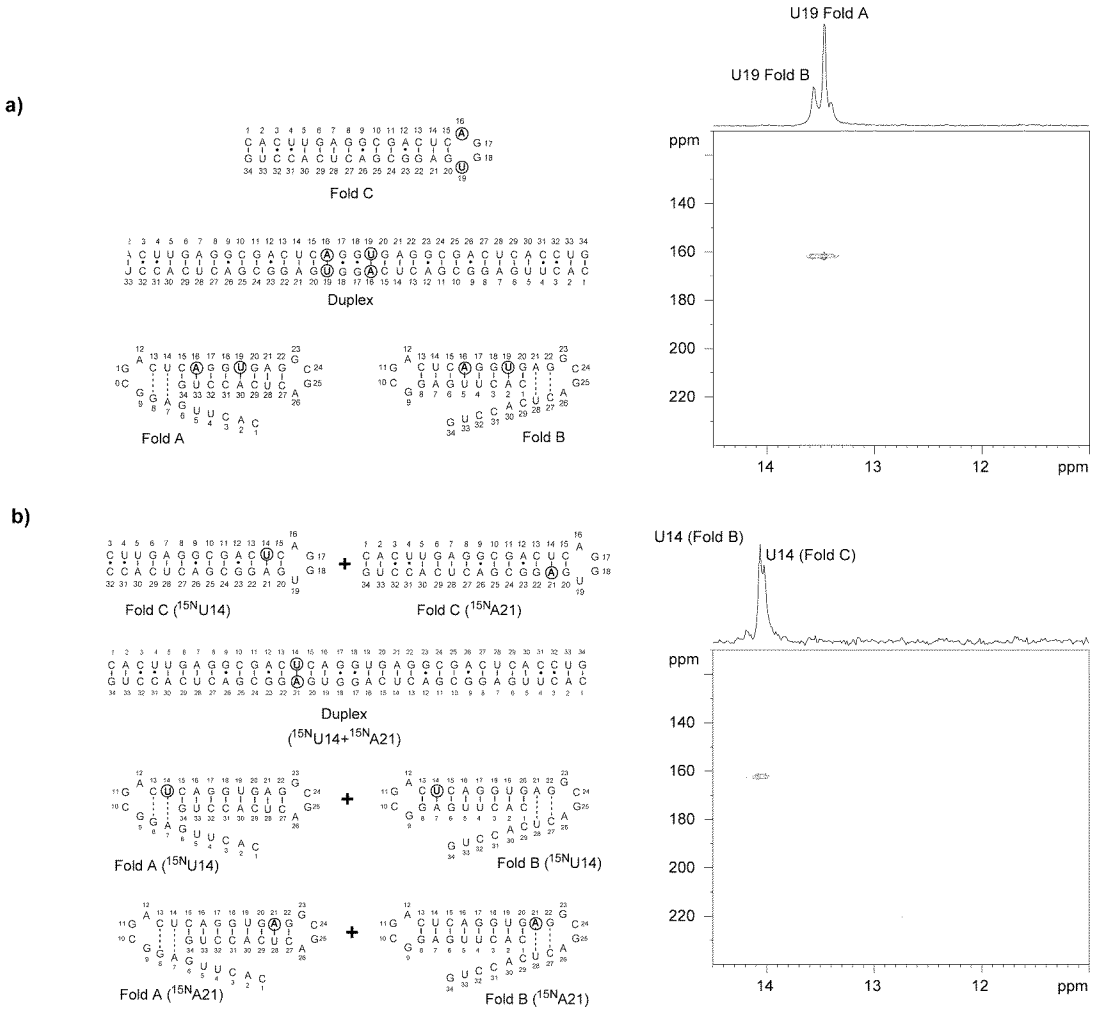

Identification of the extended hairpin fold C. The third fold which was detected by the HNN correlation experiments in Fig. 2 (main text) can either be a single hairpin (fold C) or a duplex structure. This ambiguity could be resolved by recording two additional HNN correlation experiments with the labeling patterns indicated here, which allowed us to exclude the (hypothetic) duplex structure: a) *left*: The ^{15N}U19:^{15N}A16-labeled 34mer RNA sequence forms a doubly ^{15}N-labeled U19:A16 donor/acceptor base-pair only in the (hypothetic) duplex structure; in folds A and B, U19 and A16 are paired to other nucleotides and in fold C they are located in the loop. Therefore, a HNN cross-peak between U19 and A16 should only appear for the duplex structure. *Right*: the corresponding HNN correlation spectrum does not show two cross-peaks in the ^{15}N dimension, indicating that the duplex structure is not formed. b) *left*: To further exclude the (hypothetic) duplex structure we prepared a (1:1)-mixture of the ^{15N}U14-labeled 34mer sequence and the ^{15N}A21-labeled 34mer sequence. A doubly ^{15}N-labeled donor-acceptor base pair can only form in a hetero-duplex comprising the two differently labeled sequences. *Right*: again, the corresponding HNN correlation spectrum does not show two cross-peaks in the ^{15}N dimension, thus providing strong evidence against the existence of the duplex structure.

2. Supporting Figure S2: Temperature dependence of ^{15}N-filtered 1D ^{1}H spectra

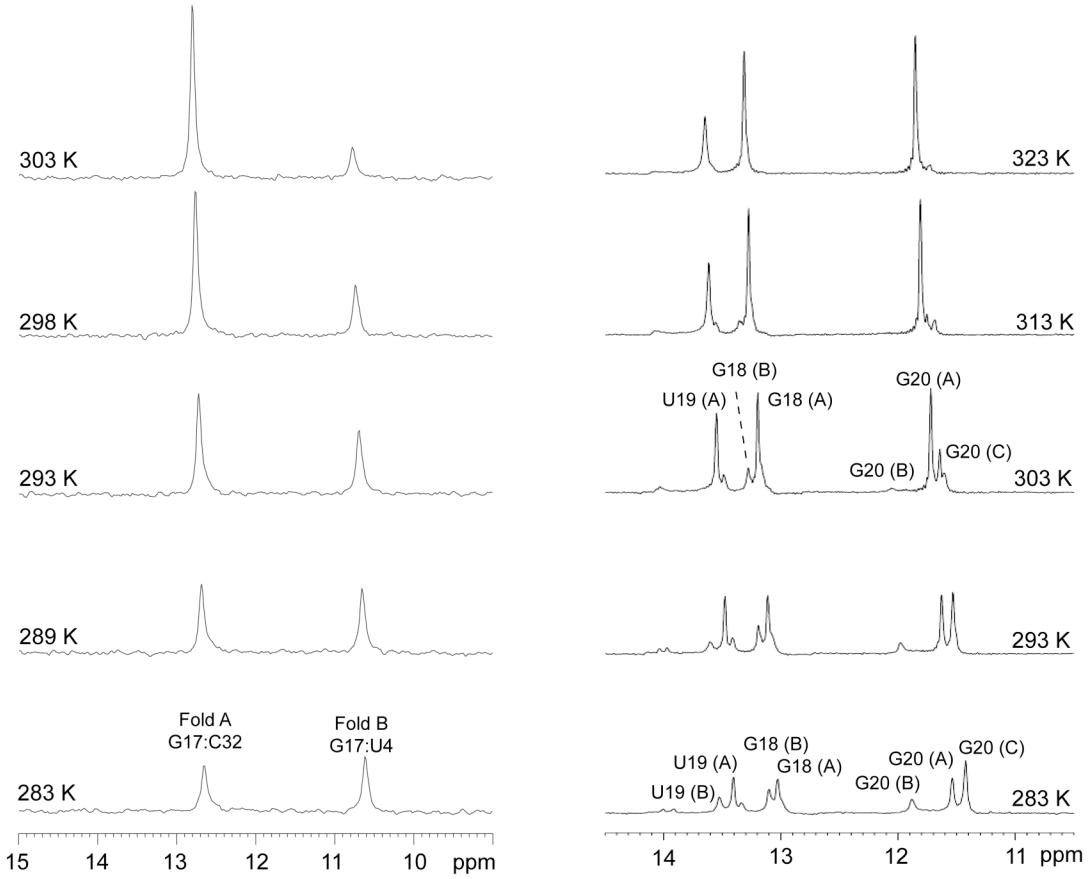

Figure S2. (*left*): Temperature dependence of ^{15}N-filtered 1D ^{1}H NMR spectra of the ^{15N}G17-labeled 34mer RNA sequence. The signals for G17:C32 (Fold A) and G17:U4 (Fold B) show how the equilibrium is shifted towards fold A with increasing temperature. (*right*): Temperature dependence of ^{15}N-filtered 1D ^{1}H NMR spectra of the ^{15N}C1, ^{15N}A2, ^{15N}C3, ^{15N}G18, ^{15N}U19, ^{15N}G20-labeled 34mer RNA sequence of Fig. 2d. Again, the equilibrium is shifted towards fold A with increasing temperature. At 293 K, folds A and C are nearly equally populated; at 323 K fold A is predominant.

3. Supporting Fig. S3a: Exchange rates obtained by selective excitation of the G17:C32 imino protons

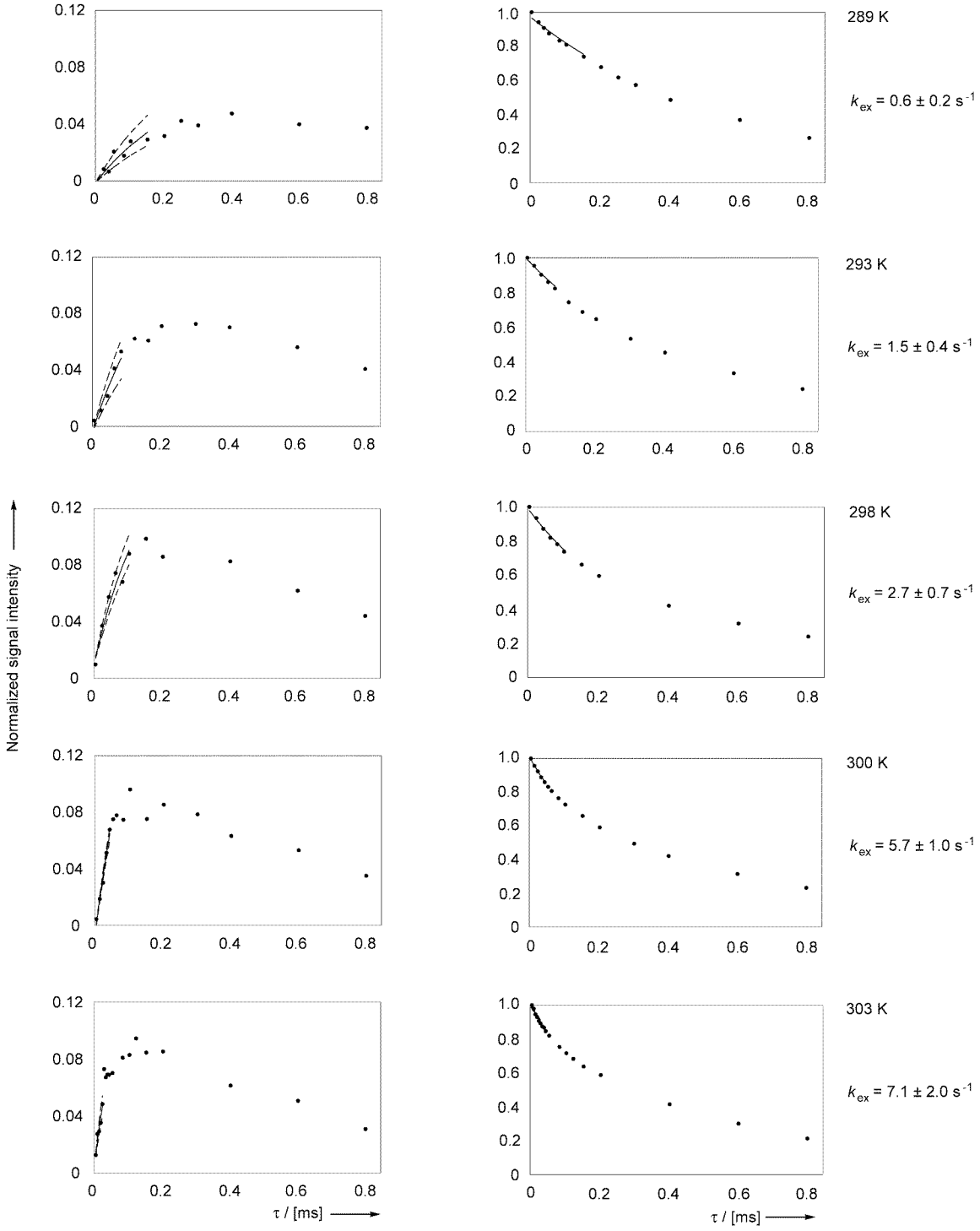

Figure S3a. Build-up and decay curves as a function of the mixing time, obtained after selective excitation of the G17:C32 imino protons at different temperatures.

Supporting Figure S3b: Exchange rates obtained by selective excitation of the G17:U4 imino protons

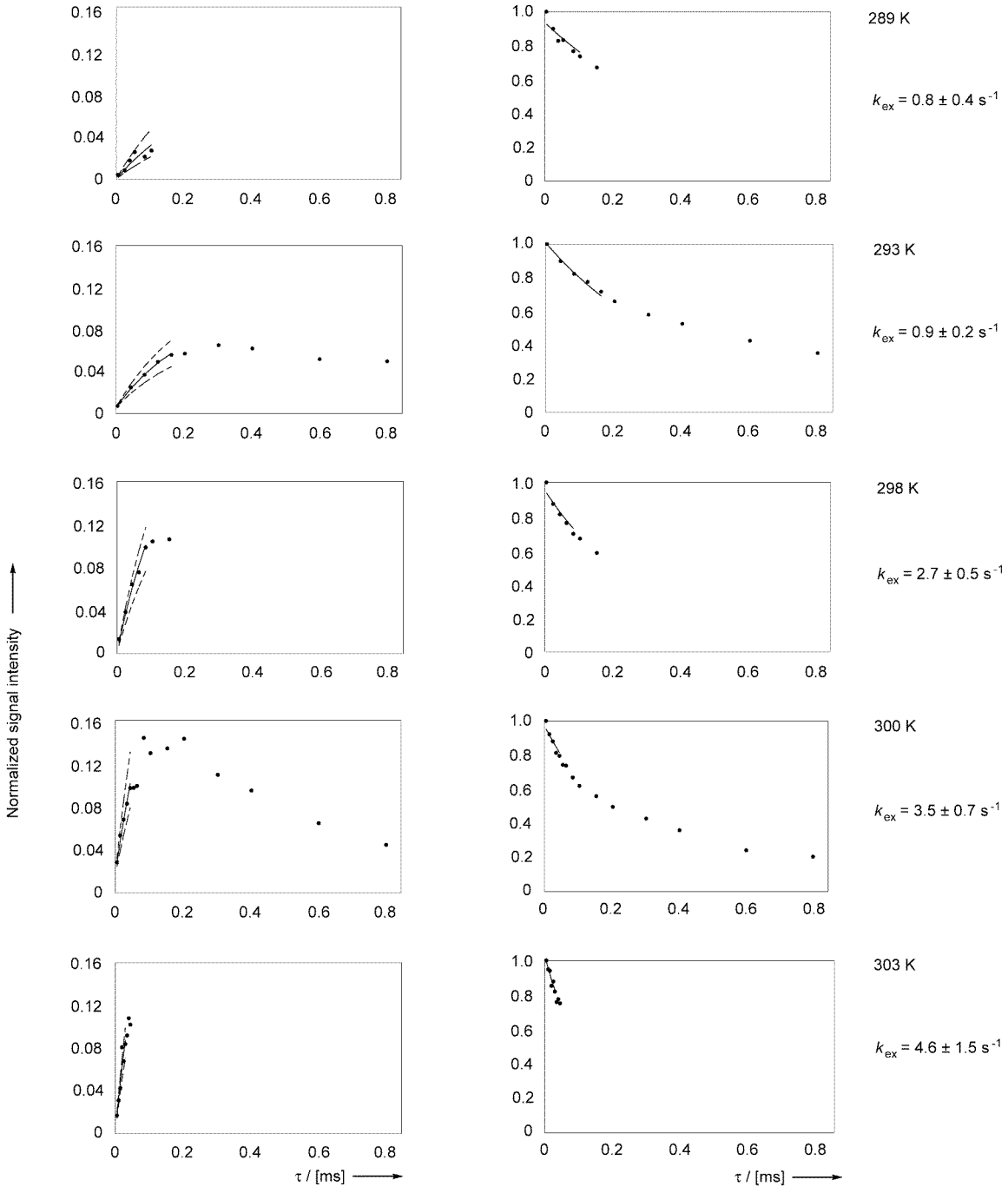

Figure S3b. Build-up and decay curves as a function of the mixing time, obtained after selective excitation of the G17:U4 imino protons at different temperatures.

4. Supporting Figure S4: Comprehensive table of all equilibrium and rate constants

a)

T [K]	K_{eq}	k_{ex}(GC) [s^{-1}]	$k_{A\rightarrow B}$(GC) [s^{-1}]	$k_{B\rightarrow A}$(GC) [s^{-1}]
289	0.8	0.6 ± 0.3	0.31 ± 0.10	0.24 ± 0.06
293	1.0	1.5 ± 0.4	0.74 ± 0.30	0.75 ± 0.20
298	1.4	2.7 ± 0.7	1.11 ± 0.40	1.58 ± 0.40
300	1.9	5.7 ± 1.0	1.94 ± 0.50	3.74 ± 1.00
303	2.4	7.1 ± 2.0	2.10 ± 0.70	4.96 ± 2.00

b)

T [K]	K_{eq}	k_{ex}(GU) [s^{-1}]	$k_{A\rightarrow B}$(GU) [s^{-1}]	$k_{B\rightarrow A}$(GU) [s^{-1}]
289	0.8	0.8 ± 0.4	0.44 ± 0.20	0.36 ± 0.20
293	1.0	0.9 ± 0.2	0.44 ± 0.10	0.45 ± 0.20
298	1.4	2.7 ± 0.5	1.20 ± 0.30	1.58 ± 0.50
300	1.9	3.5 ± 0.7	1.20 ± 0.30	2.33 ± 0.70
303	2.4	4.6 ± 1.5	1.38 ± 0.20	3.26 ± 1.20

a) Equilibrium constants K_{eq} = [A]/[B] and rate constants determined for the 34mer-RNA sequence by selective excitation of G17:C32 imino protons (a) and the G17:U4 imino protons (b).

5. Bloch-McConnell Equations

5.1. Two-state model

The equilibrium intensities that normally appear in the Bloch-McConnell equation (a: McConnell, H.M. *J. Chem Phys*. **1958**, *28*, 430-431; b: Led, J.J. *J. Magn. Res*. **1982**, *49*, 444-463) are experimentally cancelled out by phase cycling. The exchange rates were determined by fitting the signal intensities in the initial rate approximation to the solution of the following homogeneous differential equation:

$$\frac{d}{dt}\begin{pmatrix} I_A \\ I_B \end{pmatrix} = \begin{pmatrix} -R_{1,A} - k_{A\to B} & k_{B\to A} \\ k_{A\to B} & -R_{1,B} - k_{B\to A} \end{pmatrix}\begin{pmatrix} I_A \\ I_B \end{pmatrix} \qquad \text{(E1)}$$

with the rates $k_{A\to B}$ and $k_{B\to A}$ from fold A to fold B and *vice versa*, and where $R_{1,A}$ and $R_{1,B}$ are the ^{15}N longitudinal relaxation rates of the donor nitrogen nuclei in the base pairs G17:C32 (fold A) and G17:U4 (fold B), respectively. The solution is:

$$I_A(t) = \Lambda_{AA}\exp(\lambda_A t) + \Lambda_{AB}\exp(\lambda_B t)$$
$$I_B(t) = \Lambda_{BA}\exp(\lambda_A t) + \Lambda_{BB}\exp(\lambda_B t) \qquad \text{(E2)}$$

with

$$\lambda_A = -\tfrac{1}{2}(R_{1,A} + k_{A\to B} + R_{1,B} + k_{B\to A} - w)$$
$$\lambda_B = -\tfrac{1}{2}(R_{1,A} + k_{A\to B} + R_{1,B} + k_{B\to A} + w)$$
$$w = \sqrt{\left(R_{1,B} + k_{B\to A} - R_{1,A} - k_{A\to B}\right)^2 + 4k_{B\to A}k_{A\to B}}$$
$$\Lambda_{AA} = \left(\tfrac{1}{2}\left(w + R_{1,B} + k_{B\to A} - R_{1,A} - k_{A\to B}\right)I_A(0) + k_{B\to A}I_B(0)\right)\Big/w$$
$$\Lambda_{AB} = \left(\tfrac{1}{2}\left(w - R_{1,B} - k_{B\to A} + R_{1,A} + k_{A\to B}\right)I_A(0) - k_{B\to A}I_B(0)\right)\Big/w$$
$$\Lambda_{BA} = \left(-\tfrac{1}{2}\left(-w + R_{1,B} + k_{B\to A} - R_{1,A} - k_{A\to B}\right)I_B(0) + k_{A\to B}I_A(0)\right)\Big/w$$
$$\Lambda_{BB} = \left(-\tfrac{1}{2}\left(-w - R_{1,B} - k_{B\to A} + R_{1,A} + k_{A\to B}\right)I_B(0) - k_{A\to B}I_A(0)\right)\Big/w$$

5.2. Three-state model

In the 2D EXSY experiment of Fig. 5, the cross-peak intensities I_{AC} and I_{BC} do not emerge above the noise level, so that possible exchange processes between fold C and folds A and B are too slow to be detected ($k_{ex} < 0.1\ s^{-1}$).

In order to assess the potential impact of slow exchange with fold C on the apparent rate of the A→B transformation, calculations including three states were carried out. The extension of the *Bloch-McConnell* Equation E1 (see Supp. Inf. 5.1) to three states gives the following differential equation for the signal intensities:

$$\frac{d}{dt}\begin{pmatrix} I_A \\ I_B \\ I_C \end{pmatrix} = \begin{pmatrix} -R_{1,A} - k_{A\to B} - k_{A\to C} & k_{B\to A} & k_{C\to A} \\ k_{A\to B} & -R_{1,B} - k_{B\to A} - k_{B\to C} & k_{C\to B} \\ k_{A\to C} & k_{B\to C} & -R_{1,C} - k_{C\to A} - k_{C\to B} \end{pmatrix} \begin{pmatrix} I_A \\ I_B \\ I_C \end{pmatrix} \quad \text{(E3)}$$

or

$$\frac{d}{dt} I = -\hat{P}\, I \quad \text{(E4)}$$

Equation E4 was solved by stepwise integration

$$I(t+\tau) = e^{-\hat{P}\tau}\, I(t) \quad \text{(E5)}$$

where τ is the length of each step. Calculations were carried out under the following assumptions. The relative population of fold C was set to $p_C = 0.35$ and the relative populations of A and B were set to $p_A = p_B = 0.325$, in agreement with the previously determined equilibrium constant K_{AB}. The rate constants $k_{A\to C}$ and $k_{B\to C}$ were set to the worst-case upper limit of 0.1 s^{-1} (estimated from the absence of cross-peaks above the noise level of the 2D EXSY experiment in Fig. 5), which represents the highest possible value for these exchange rates. The rate constants $k_{C\to A}$ and $k_{C\to B}$ were calculated according to $k_{C\to A} = k_{A\to C}\, p_A/p_C$ and $k_{C\to B} = k_{B\to C}\, p_B/p_C$. The remaining rate constants $k_{A\to B}$ = 1.15 s^{-1} and $k_{B\to A}$ = 1.58 s^{-1} have been determined previously using the two-state *Bloch-McConnell* equation (see Supp. Table S4).

Result: The exchange rates $k_{A\to B}$ and $k_{B\to A}$ between fold A and B resulting from this calculation differ from the corresponding rates previously determined by a two-site model by less than 1%.